Mon. Not. R. Astron. Soc. **000**, ??–?? (2008) Printed 21 January 2008 (MN LATEX style file v2.2)

Deep Analyses of Nulling in Arecibo Pulsars Reveal Further Periodic Behavior

Jeffrey L. Herfindal and Joanna M. Rankin
Physics Department, University of Vermont, Burlington, VT 05405⋆

Accepted 2008 month day. Received 2008 month day; in original form 2008 month day

ABSTRACT
Sensitive Arecibo observations provide an unprecedented ability to detect nulls for an accurate pulse-modulation quelling (PMQ) analysis. We demonstrate that a number of conal pulsars show "periodic nulling" similar to the phenomenon found earlier in pulsar B1133+16.

Key words: miscellaneous – methods: — data analysis – pulsars: general

1 INTRODUCTION

The complex inner workings of the pulsar emission mechanism still remain something of a mystery four decades after their discovery. Pulsar emission is both difficult and fascinating, in part, because of its prominent modulation phenomena—in particular the "big three" effects of subpulse drifting, "mode" changing, and the pulse "nulling" that is the subject of this paper.

The nulling phenomenon has been very perplexing since first identified by Backer (1970), because the nulls affected all components, even interpulses, and were simultaneous at all frequencies. Nulls thus appeared to represent a temporary cessation of the pulsar emission process, but strangely "memory" was observed across nulls in some cases (Page 1973). Null fractions (NF) were computed for many of the known pulsars, and found to range from less than 1% up to 70% or so; but some half the stars appear not to null at all. The first systematic study of such null fractions was made by Ritchings (1976), who found a correlation between the NF and a pulsar's spin-down age τ. Ten years later, Rankin (1986) showed that while old pulsars null more than young ones, many old pulsars do not null at all.

Ever more dramatic cases of extreme nulling—that is, apparent episodes of activity and inactivity—have been discovered over the intervening two decades: *e.g.*, those of B0826–34 last for hours (Durdin *et al.* 1979); B1944+17 nulls 70% of the time (Deich *et al.* 1986); and B1931+24 seems to cycle semi-periodically on a time scale of a few weeks (Kramer *et al.* 2006).

Evidence has steadily accrued over the last few years that the nulls in many pulsars are not random turn-offs: the subpulse "memory" across nulls in B0809+74 closely associates them with the star's drift (van Leeuwen *et al.* 2002, 2003); evidence of sputtering emission during nulls has been identified in both B0818–13 (Janssen & van Leeuwen 2004) and B1237+25 (Srostlik & Rankin 2005); almost all the nulls occur in one mode in B2303+30 (Redman *et al.* 2005); in B0834+06 the nulls tend to occur on the weak phase of the star's alternate-pulse modulation cycle (Rankin & Wright 2007a); and finally the nulls in J1819+1305 exhibit a strong 57-stellar-rotation-period cyclicity (Rankin & Wright 2007b). These circumstances strongly suggest that nulls, in many cases, represent "empty" sightline traverses through a regularly rotating "carousel" subbeam system (*e.g.*, Deshpande & Rankin 2001).

In a recent paper (Herfindal & Rankin 2007; hereafter Paper I), we identified evidence for periodic nulling in pulsar B1133+16, a pulsar which exhibits no regular subpulse modulation. The nulls could be distinguished with great certainty in this star, and we then applied a straightforward method of filling the non-null pulses with the appropriately scaled-down average profile. This pulse-modulation quelling (hereafter PMQ) technique then confirmed that star's low frequency modulation feature was associated with its nulls. Here, the implication is that this star's nulls are produced by a relatively stable, but irregular and sparsely filled carousel-beam system whose rotation gives a rough periodicity to "empty" sightline passes. Such an interpretation may also explain Bhat *et al.*'s (2007) result that B1133+16's null pulses are not strictly simultaneous at all frequencies. They found about a 5% excess of nulls at meter wavelengths, and this may result from the star's larger conal emission pattern here.

These various current results lend new importance to understanding pulsar nulling more fully. Carousel-related "pseudonulls" may occur widely and explain much, but in certain stars the evidence is very strong that their nulls represent a cessation of their emission (*e.g.*, B1931+24), so at least two different types of nulls are implied. Nulling

⋆ J.Herfindal@gmail.com; Joanna.Rankin@uvm.edu

is also closely associated with mode changing (*e.g.*, Wang *et al.* 2007), and the recently discovered rotating-radio transients (RRATs) naturally raise questions about the nature of such pulsars' long dormancies between their sporadic powerful bursts (McLaughlin *et al.* 2005).

Here we continue the analytical effort begun in Paper I—that is, applying the PMQ method to a small population of pulsars with conal profiles in order to test its efficacy and interpret its results in a larger context. Our Arecibo observations and analysis methods are briefly discussed in §2 and our results for each pulsar in §3. In §4 we summarize and discuss the results overall.

2 OBSERVATIONS & METHODS

All of the observations were carried out using the 305-meter Arecibo Telescope in Puerto Rico. Observations were conducted in the P band at 327 MHz. They used the same correction methods and instrumental techniques as in Paper I. Table 1 gives the resolution, length, and date of each observation.

Longitude-resolved fluctuation spectra (hereafter LRF) of the total power component (Stokes I) were computed for all of the observations in Table 1 using Fourier transforms of length 256[1]. Figure **??** shows the LRF spectra for pulsar B2034+19 with the aggregate intensity (middle panel of the right column) showing a clear 57±6 P_1 feature.[2]

The null histogram for pulsar B2034+19 is shown in Figure **??**. Notice the strong presence of pulses with zero (or near zero) aggregate intensity. However, note that the distribution is continuous between the pulses and nulls, frustrating any possibility of delineating the two populations positively. The dotted line represents the optimal boundary between nulls and pulses, corresponding to PSR B2034+19; 44% of the pulses fall below this threshold. Suitable pulse-intensity histograms were plotted for each observation to determine a plausible null threshold.

Pulse modulation quelling (hereafter PMQ) was preformed on each observation by computing a binary series of nulls and pulses, particular to each observation. To get this, the null threshold from the pulse-intesity histograms was compared to each pulse, within the same window, in order to determine if it was a pulse or null. A new pulse sequence was created corresponding to the natural pulse sequence by substituting a scaled-down average profile for pulses and zero intensity for the "null" pulses. The lowest panel of the right column in Fig. **??** shows the LRF of the PMQ pulse sequence for pulsar B2034+19. Notice that the same low frequency feature persists!

3 INDIVIDUAL PULSAR PARAMETERS

B0301+19: This pulsar has been found to have straight drift bands in both components on the pulse–stack by Schönhardt & Sieber (1973). Weltevrede *et al.* (2006, 2007; hereafter W0607), during their two-dimensional Fourier series (hereafter 2DFS) analysis, found the trailing component exhibits a broad drift feature with a much higher P_3 value than in the leading component. The LRF shows two prominent low frequency features which have a much higher value then any of the P_3 values reported. The highest feature is only prominent in the trailing component (this may be due to the sporadic nature of the trailing component) with the 51 ± 5 P_1 feature appearing in both components. After PMQ analysis only the 51 period feature remains. Rankin (1986) found a null fraction around 10%. The null histograms show a slightly larger null fraction, on order of 13%.

B0525+21: Backer (1973) found if emission occurs in component II then it can be predicted, reliably, that the next subpulses will be in component I. He also found that the most prominent feature is at 0.025 cycles/P_1 (40 P_1) and that it is present at all longitudes across the pulse. Taylor *et al.* (1975) found a very weak preference for negative subpulse drift in adjacent pulses, but it is almost equal to a positive subpulse drift. Recently W0607 found the trailing component shows a drift feature with opposite drift direction (at 21-cm), while there is evidence for a preferred negative drift direction in the leading component at 21-cm and 92-cm. They also confirmed

Table 1. Observational parameters.

Pulsar	Date (m d^{-1} yr^{-1})	Length (pulses)	Resolution (°/sample)
B0045+33	01/07/2005	1085	0.30
B0301+19	01/08/2005	1729	0.19
B0525+21	10/04/2003	636	0.35
	10/07/2006	961[a]	0.35
J0540+32	10/07/2006	1145	0.48
B0751+32	10/04/2003	1248	0.35
	10/07/2006	2080	0.35
B0823+26	10/04/2003	3392	0.35
B0834+06	10/05/2003	3789	0.35
	05/06/2006	1920	0.35
B1237+25	07/12/2003	2340	0.35
	07/13/2003	5094	0.35
	07/20/2003	4542	0.35
	01/08/2005	5209	0.13
J1649+2533	01/06/2005	1044	0.36
	02/12/2006	2818	0.36
J1819+1305	02/12/2006	3394	0.51
B1831-00	01/07/2005	1151	0.71
B1839+09	01/07/2005	1573	0.48
B1848+12	10/19/2003	2074	0.15
	08/19/2006	1037	0.48
B1918+19	02/12/2006	3946	0.39
B2034+19	01/07/2005	1676	0.36
B2122+13	01/08/2005	1038	0.36
B2303+30	10/07/2003	1526	0.23
B2315+21	10/07/2003	622	0.35
	01/07/2005	2491	0.26

[a] The last 121 pulses of this observation were ignored due to noticeable interference.

[1] Pulsar B0525+21, observation dated 2003 October 4, used a FFT of length 128. Pulsars B2303+30 and J0540+32 both used a FFT of length 512.

[2] P_1 is that particular pulsar's period.

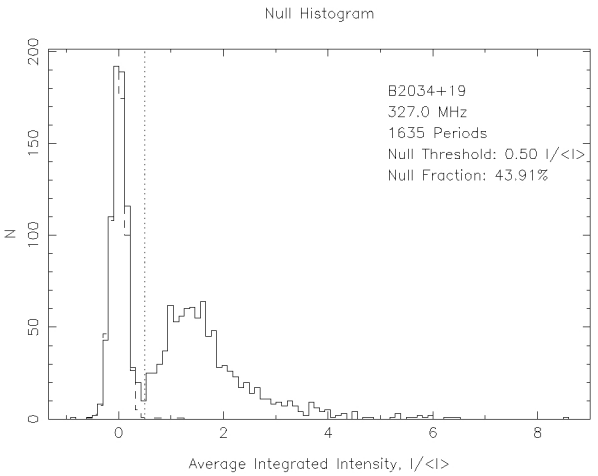

Figure 1. Null histogram for the pulsar B2034+19. The integrated-intensity distribution of the pulses (solid line) and that of the off-pulse region (dashed line) are plotted. The vertical dotted line represents an integrated intensity limit of 0.50 $<I>$ to distinguish the nulls. Notice the null distribution is contiguous with that of the pulses frustrating any attempts to decisively measure the null fraction. Forty one (41) pulses were ignored due to bad baselines.

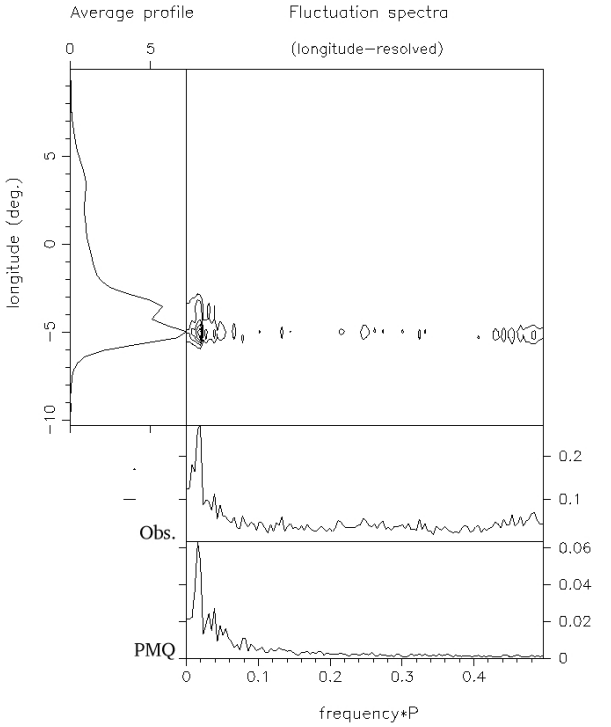

Figure 2. Typical LRF plot for pulsar B2034+19 computed in total power (Stokes I). The main panel gives the spectra according to the average profile in the left panel, and the integrated spectrum is shown in the middle panel, right column. LRF spectra of the artificial "PMQ" PS corresponding to this pulsar is in the bottom panel. Most pulse modulation was quelled by substituting a scaled-down average profile for the pulses while zero intensity was substituted for detected nulls (see text). Here, as for most of the observations, an FFT length of 256 was used.

a P_3 around 3.8 P_1. The LRF features vary between the observations with only one remaining feature after PMQ analysis. The 4-odd P_1 drift feature is only seen in the longer of the observations in the normal LRF. The null histograms show a continuous distribution between that of the pulses and the nulls, giving a varying null fraction between the observations. These null fractions are consistent with Ritchings (1976) of 25%.

J0540+32: This newly discover pulsar was found during the Arecibo Pulsar survey using the ALFA (Cordes *et al.* 2006). This pulsar has a clear separation between the null and pulse distributions with 54% percent of the pulses falling below our null threshold. There is a distinct very low frequency feature at 256±64 P_1. The PMQ spectra shows the same feature with another harmonic feature at 85±7 P_1.

B0751+32: At 430 MHz Backus (1981) identified a preference for negative drift in this pulsar; recently, W0607 found the leading and trailing components show a low frequency feature at 60±20 P_1 and 70±10 P_1, respectfully (at 92-cm). Once the observations underwent Fourier transforms, the LRF's revealed that the low frequency feature changes slightly between our observations. Nevertheless, after PMQ analysis the main features in the original LRF's remain. Nulling in B0751+32 occurs around 34% (Backus, 1981). The null fraction from the pulse-intensity distribution histograms changes slightly but is consistent with Backus's results.

B0834+06: Taylor *et al.* (1969) found a strong response at 0.462 cycles/P_1 (2.16 P_1), confirmed by Slee & Mulhall (1970), Sutton *et al.* (1970) identified it as a drifting feature, Backer (1973), Taylor (1975) found a preference for positive subpulse drift, and recently by Asgekar & Deshpande (2005) and W0607 confirmed the drifting feature's measurement of 2.2P_1. Rankin & Wright (2007a) showed the nulls are not randomly distributed, occurring in a periodic matter. The LRFs of these observations have a clear feature around 2.16 P_1 which is conserved after PMQ. An unexpected feature was found after PMQ analysis of the longer observation at 16 P_1. A null fraction of around 7.1% was found by Ritchings (1976); Rankin & Wright (2007a) found that no more then 9% of pulses are nulls. These observations have very distinct null–pulse distributions resulting in accurate null fractions which confirm these previous results.

J1649+2533: This pulsar was found to have a null fraction of 30% by Lewandowski *et al.* (2004). The null fractions in these observations are slightly lower (on order of 21%). Lewandowski *et al.* also measured a $P_3 = 2.2$ P_1; both of the observations show this feature towards the outer edges of the profile, with a clear separation in the middle. After PMQ analysis, only the 27-odd P_1 feature remains.

J1819+1305: A very clear feature at 57±6 P_1 in the LRF is spread across the whole pulse with a slight absents in the middle. This feature remains as prominent after PMQ analysis. The null histogram is a continuous distribution deterring any possibility of an accurate measurement of "null" pulses.

B1839+09: W0607 confirmed the result (at 21 and 92 cm) found by Backus (1981); stating that there is no preference in the drift direction for the subpulse modu-

Table 2. Observed low frequency feature(s), features after PMQ, and null fractions.

J2000 name	B1950 name	Length (pulses)	NF (per cent)	LRF Feature(s) (P_1)	PMQ Feature (P_1)	Figure
J0304+1932	B0301+19	1729	15	128 ± 32	—	Fig. A.??
				51 ± 5	51 ± 5	
J0528+2200	B0525+21	636	22	51 ± 10	43 ± 7	Fig. A.??
		961	32	39 ± 3	—	
				28 ± 2	—	
				22 ± 1	23 ± 1	
				4.57 ± 0.04	—	
J0540+32	—	1145	54	256 ± 64	256 ± 64	Fig. A.??
J0754+3231	B0751+32	1248	36	51 ± 5	51 ± 5	Fig. A.??
		2080	40	64 ± 8	73 ± 10	
J0837+0610	B0834+06	3789	9	2.17 ± 0.01	2.18 ± 0.01	Fig. A.??
				—	16 ± 1	
		1920	9	2.15 ± 0.01	2.15 ± 0.01	
J1649+2533	—	1044	21	64 ± 8	—	Fig. A.??
				28 ± 2	28 ± 2	
				2.5 ± 0.1	—	
		2818	27	57 ± 6	57 ± 6	
				26 ± 1	26 ± 1	
				2.5 ± 0.1	—	
J1819+1305	—	3394	46	57 ± 6	64 ± 8	Fig. A.??
J1841+0912	B1839+09	1573	3	37 ± 3	37 ± 3	Fig. A.??
				28 ± 2	—	
J1921+1948	B1918+19	3946	9	85 ± 14	85 ± 14	Fig. A.??
				—	43 ± 4	
J2037+1942	B2034+19	1676	44	57 ± 6	57 ± 6	Figs. ??,??
J2305+3100	B2303+30	1526	11	102 ± 20	128 ± 32	Fig. A.??
				—	64 ± 8	
				37 ± 3	37 ± 3	

lation. The LRF for this observation shows a clear feature at 37±3 P_1, which also remains after PMQ was performed. The null histogram shows clearly that the pulse distribution trails off into the null distribution, resulting in a null fraction of 2%.

B1918+19: Four drifting modes identified by Hankins & Wolszczan (1987). This pulsar has a continuous distribution between the "null" and pulse distributions in the pulse- energy histogram. A conservative null threshold was chosen, correspondingly 9% of these pulses fall below this threshold. The LRF shows a strong low- frequency feature at 85±14 P_1. This feature persists after PMQ analysis.

B2034+19: This pulsar has a clear null and pulse distribution in the pulse-intensity histogram. The LRF shows a clear feature at 57±6 P_1 which remains after PMQ analysis.

B2303+30: Redman *et al.* (2005) found two modes in this pulsar with almost all of the nulls come about in the 'Q' (quiescent) mode. 11% of the pulses in this pulsar fall below the null threshold in the pulse-energy histograms. The LRF shows two low frequency features: one at 102±20 P_1 with the other at 37±3 P_1. Both of these features remain after PMQ analysis.

Table 3. Observed null fractions of "featureless" pulsars.

J2000 name	B1950 name	Length (pulses)	NF (per cent)
J0048+3412	B0045+33	1085	22
J0826+2637	B0823+26	3392	7
J1239+2453	B1237+25	2340	5
		5094	6
		4542	6
		5209	5
J1834-0010	B1831–00	1151	3
J1851+1259	B1848+12	2074	54
		1037	50
J2124+1407	B2122+13	1038	27
J2317+2149	B2315+21	622	2
		2491	2

4 DISCUSSION

Our surprise in Paper I was that the PMQ analysis associated B1133+16's low frequency feature so clearly with its *nulls*! In this larger effort, we are no longer surprised to find abundant evidence for null-related periodicities in this population of conal dominated pulsars. We do, however, find pulsars whose nulls show no obvious periodicity

as well as cases where PMQ reveals several, probably harmonically related, periodicities.

Specifically, the PMQ analysis did not always identify null periodicity. Table 3 lists seven pulsars which clearly have a null fraction but do not, except for B1237+25 & B1831–00, have a clear LRF feature. These seven pulsars tend to produce either very broad features or featureless ("random") PMQ LRF spectra. These non-definitive results could come about because a pulsar: i) has several different drift modes; ii) an irregular carousel rotation rate; iii) an unfavorable sight-line traverse across the edge of the carousel; or iv) has nulls that are completely random.

In all cases the pulse-energy distributions were continuous with those of the null distributions. Strangely, we have yet to encounter any example of a pulsar whose pulses and nulls are fully disjoint.

The results of this paper amplify the evidence reviewed above to the effect that many pulsar nulls are neither random nor complete turn-offs. Other recent evidence (*e.g.*, B1931+24), however, all but confirms absolutely that some pulsar nulls do represent a complete or almost complete cessation of the emission. The conclusion then can hardly be escaped that pulsar nulls are of at least two distinct types. And the recently discovered RRATs then reverse the traditional null question: "How can an electrodynamic system which is almost always in the null state then flash very occasionally into brilliance?"

ACKNOWLEDGMENTS

Portions of this work were carried out with support from US National Science Foundation Grant AST 99-87654. Arecibo Observatory is operated by Cornell University under contract to the US NSF. This work used the NASA ADS system.

REFERENCES

AD05 Asgekar, A., & Deshpande, A.A, *MNRAS*, 2005, 357, 1105
Backer, D.C., 1970, *Nature*, 228, 42
Backer, D. C. 1973, *Ap.J.*, 182, 245
Backus, P. R. 1981 Ph.D. Thesis, The University of Massachusetts
Bhat, N.D.R., Gupta, Y., Kramer, M., Karastergiou, A., Lyne, A.G., & Johnston, S. 2007, *A&A*, 462, 257
Cordes, J.M., Freire, P.C.C., Lorimer, D.R., *et al.* 2006, *Ap.J.*, 637, 446
Deshpande, A.A., Rankin, J.M., 2001, *MNRAS*, 322, 438
Deich, W.T.S., Cordes, J. M., Hankins, T. H., & Rankin, J. M. 1986, *Ap.J.*, 300, 540
Durdin, J. M., Large, M. I., Little, A. G., Manchester, R. N., Lyne, A. G., & Taylor, J. H. 1979, *MNRAS*, 186, 39
Hankins, T.H. & Wolszczan, A., 1987, *Ap.J.*, 318, 410
Herfindal, J. L., Rankin, J. M. 2007 *MNRAS*, 380, 430
Janssen, G.H., van Leeuwen, A.G.J., 2004, *A&A*, 425, 255
Kramer, M., Lyne, A. G., OBrien, J. T., Jordan, C. A., & Lorimer, D. R. 2006, Science, 312, 549
Lewandowski, W., Wolszczan, A., Feiler, G., *et al.* 2004, *Ap.J.*, 600 905
van Leeuwen, A.G.J., Kouwenhoven, M.L.A., Ramachandran, R., Rankin, J. M., & Stappers, B. W. 2002, *A&A*, 387, 169
van Leeuwen, A.G.J., Stappers, B. W., Ramachandran, R., & Rankin, J. M. 2003, *A&A*, 399, 223
McLaughlin, M.A., Lyne, A.G., Lorimer, D.R., Kramer, M., *et al.* 2006 *Nature*, 439, 817
Page, C.G., 1973, *MNRAS*, 163, 29
Rankin, J.M., 1986, *Ap.J.*, 301, 901
Rankin, J. M. & Wright, G.A.E. 2007a, *MNRAS*, 379, 507
Rankin, J. M. & Wright, G.A.E. 2007b, *MNRAS*, in press
Redman, S.R., Wright, G.A.E., Rankin, J.M., 2005, *MNRAS*, 357, 859
Ritchings, R.T. 1976, *MNRAS*, 176, 249
Schönhardt, R. E. & Sieber, W. 1973 Astrophys. Lett., 14, 61
Slee, O.B., Mulhall, P.S., 1970, Proc. Astr. Soc. Australia, 1, 322
Srostlik, Z. & Rankin, J.M., 2005, *MNRAS*, 362, 1121
Sutton J. M., Staelin, D. H., Price, R. M., & Weimer, R. 1970, *Ap.J.*, 159, 89
Taylor, J. H., Jura, M., Huguenin, G. R. 1969 *Nature*, 223, 797
Taylor, J. H., Manchester, R. N., Huguenin, G. R. 1975, *Ap.J.*, 195, 513
Wang, N., Manchester, R. N., & Johnston, S. 2007, *MNRAS*, 377, 1383
Weltevrede, P., Edwards, R. T., & Stappers, B. 2006, *A&A*, 445, 243
Weltevrede, P., Stappers, B. W., & Edwards, R. T. 2007, *A&A*, 469, 607

This paper has been typeset from a TEX/ LATEX file prepared by the author.

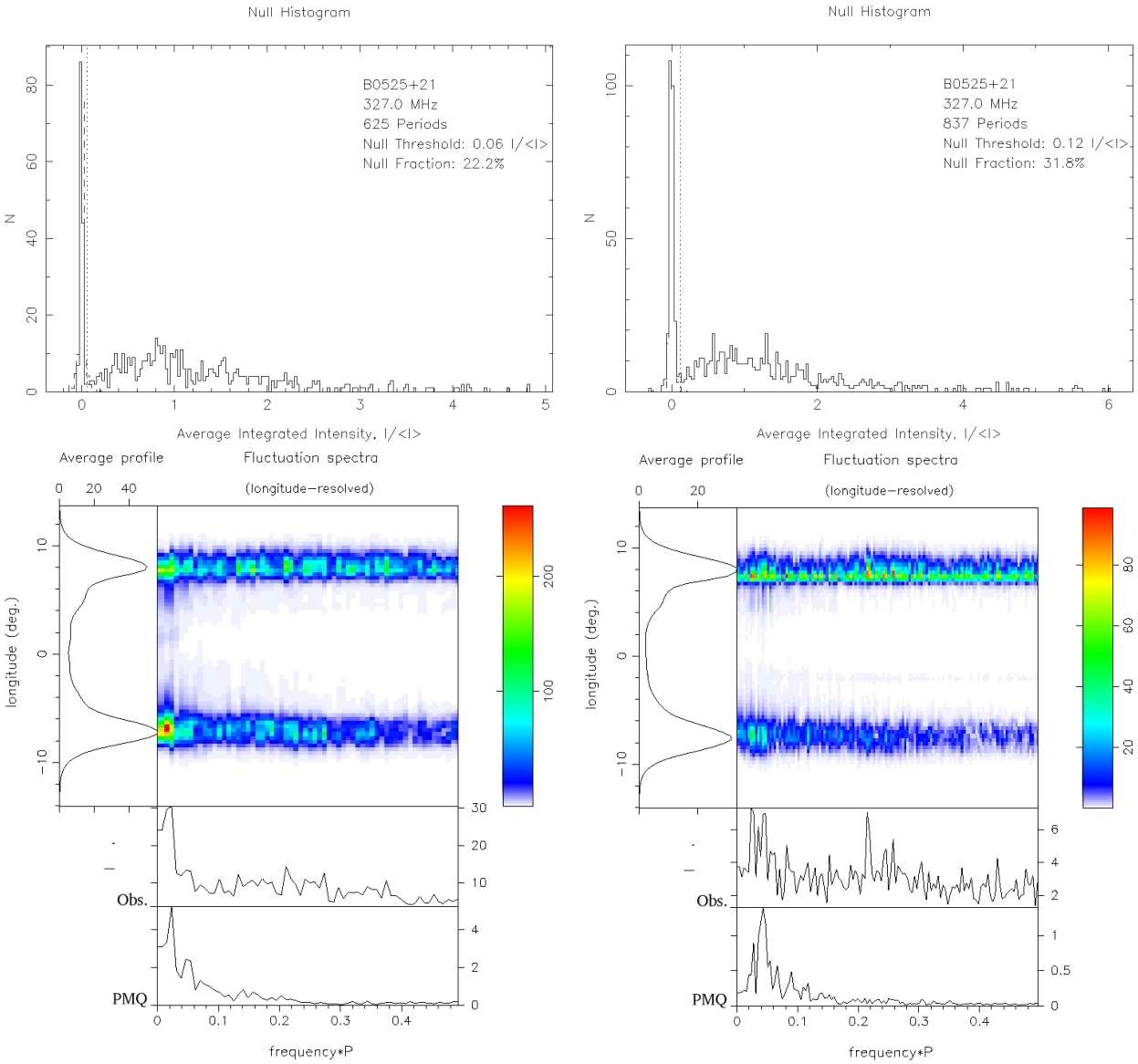

Figure 1. The top row shows typical pulse-energy histograms. The bottom rows show the average profile in the left panel, and in the right column: the LRF spectra in the top panel, the aggregate LRF spectra in the center, and the PMQ LRF aggregate spectra at the bottom. Pulsar B0525+21 is shown with the observation dated 04 October 2003 on the left, 07 October 2006 on the right.

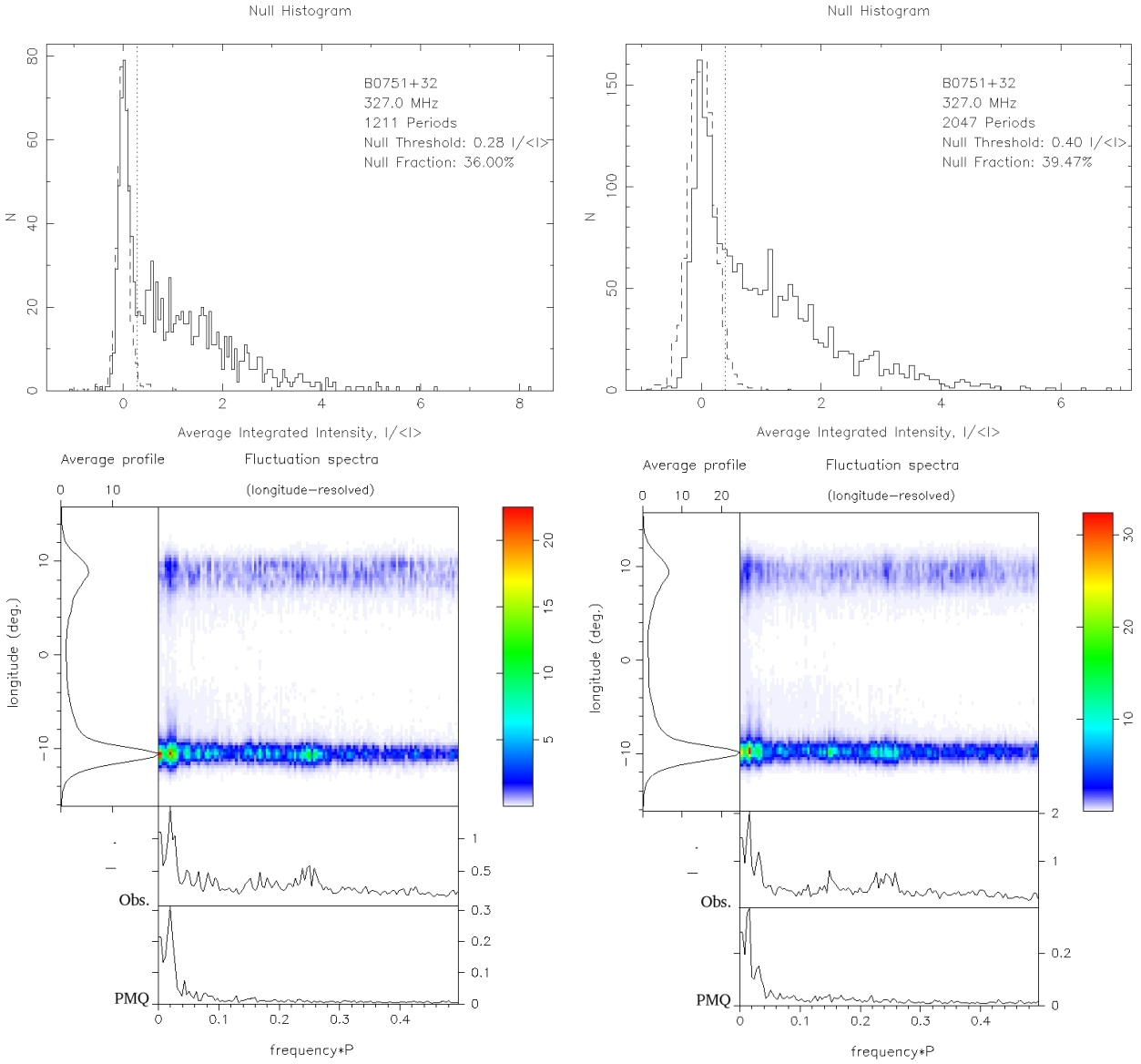

Figure 2. The top row shows typical pulse-energy histograms. The bottom rows show the average profile in the left panel, and in the right column: the LRF spectra in the top panel, the aggregate LRF spectra in the center, and the PMQ LRF aggregate spectra at the bottom. Pulsar B0751+32 is shown with the observation dated 04 October 2003 on the left, 07 October 2006 on the right.

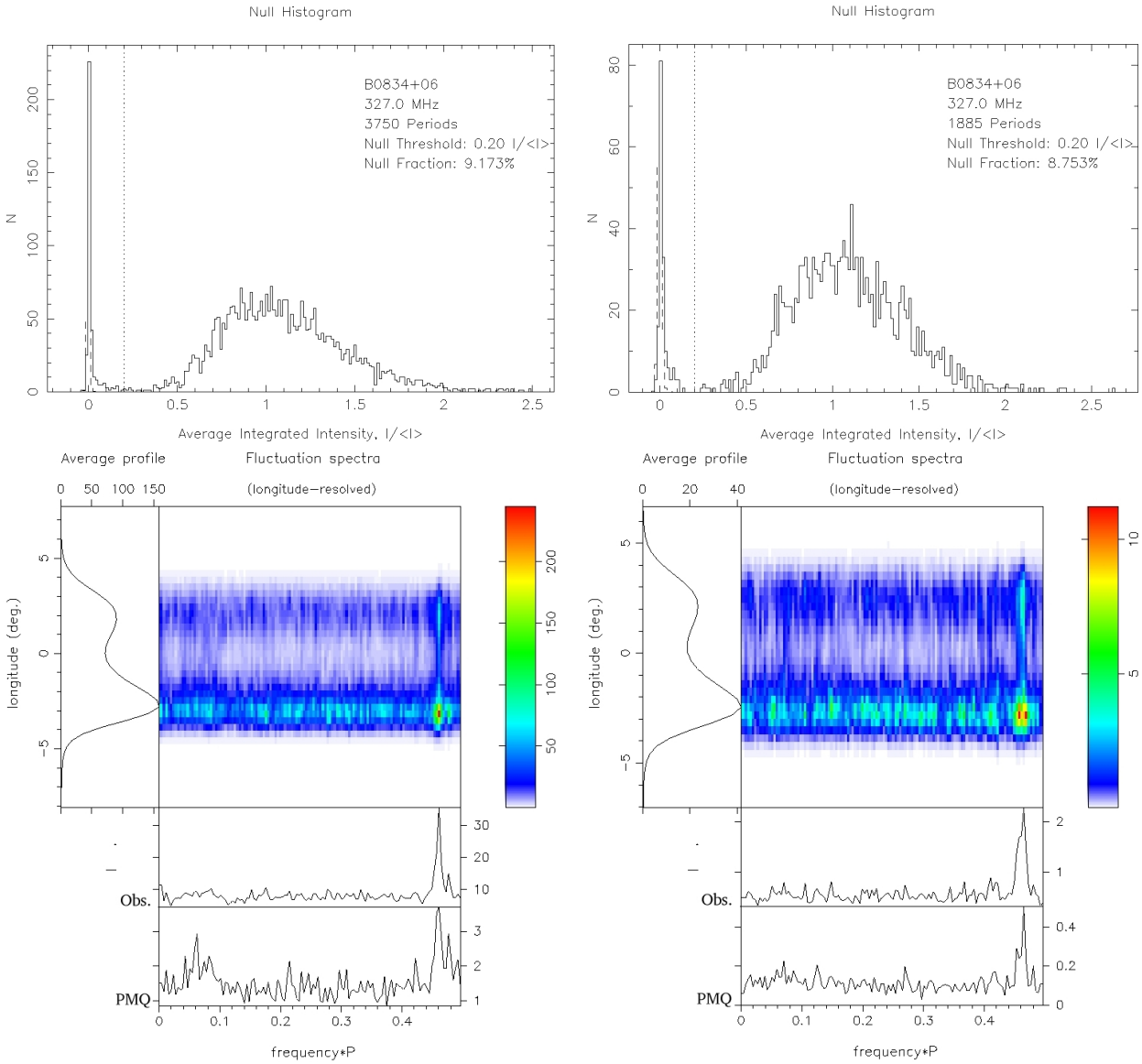

Figure 3. The top row shows typical pulse-energy histograms. The bottom rows show the average profile in the left panel, and in the right column: the LRF spectra in the top panel, the aggregate LRF spectra in the center, and the PMQ LRF aggregate spectra at the bottom. Pulsar B0834+10 is shown with the observation dated 05 October 2003 on the left, 06 May 2006 on the right.

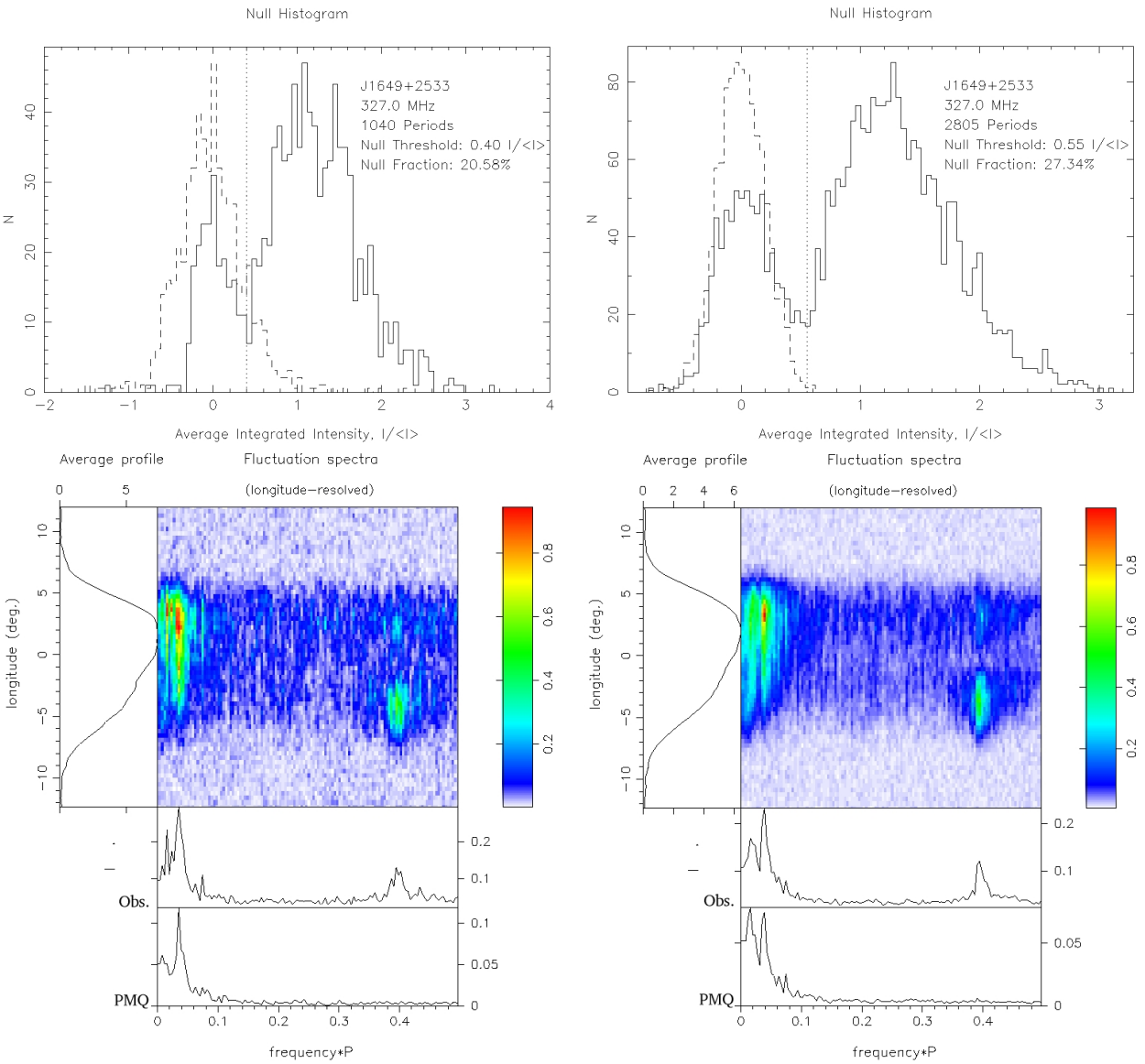

Figure 4. The top row shows typical pulse-energy histograms. The bottom rows show the average profile in the left panel, and in the right column: the LRF spectra in the top panel, the aggregate LRF spectra in the center, and the PMQ LRF aggregate spectra at the bottom. Pulsar J1649+2533 is shown with the observation dated 06 January 2005 on the left, 12 February 2006 on the right.

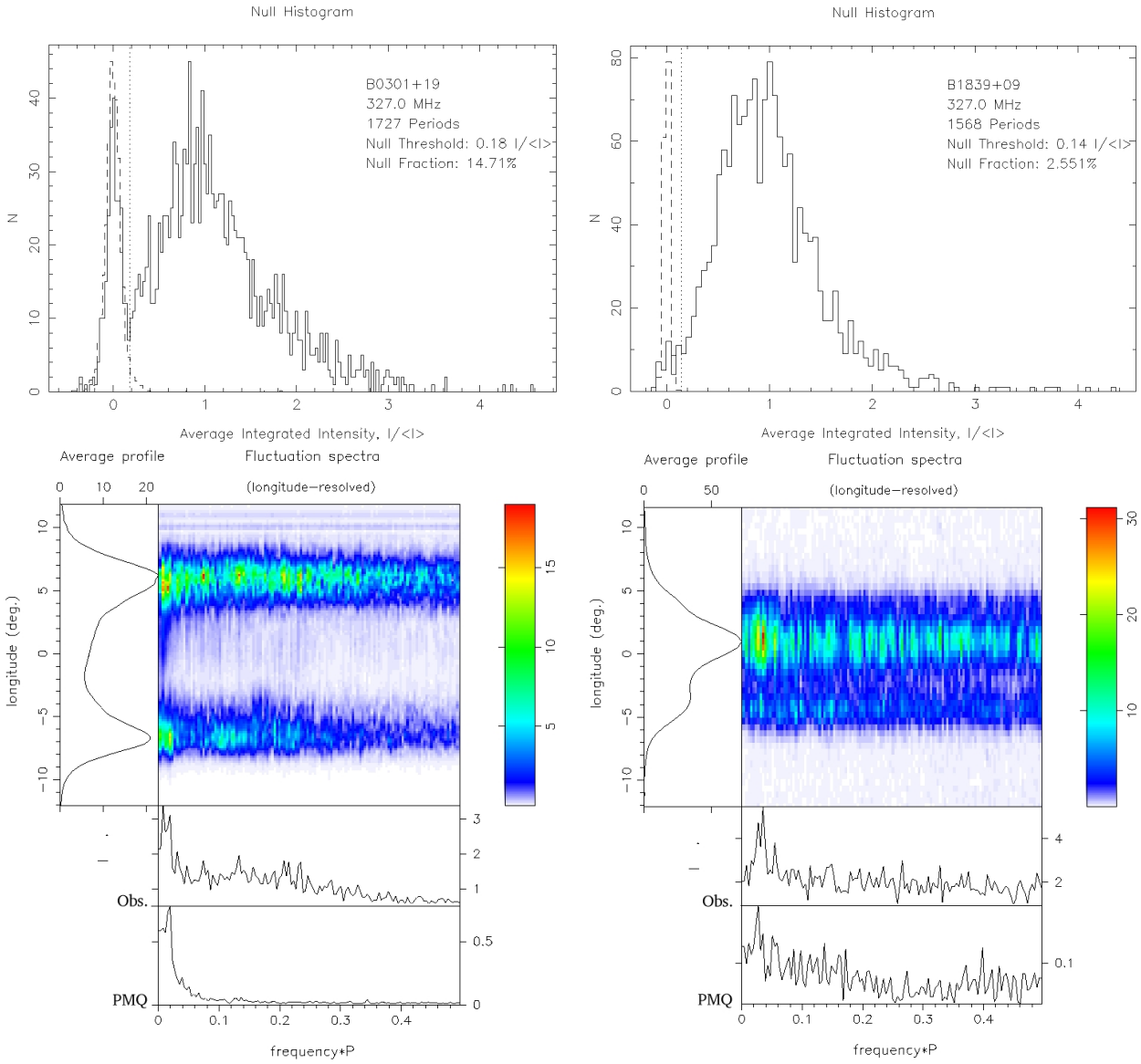

Figure 5. The top row shows typical pulse-energy histograms. The bottom rows show the average profile in the left panel, and in the right column: the LRF spectra in the top panel, the aggregate LRF spectra in the center, and the PMQ LRF aggregate spectra at the bottom. Pulsar B0301+19 on the left, B1839+09 on the right

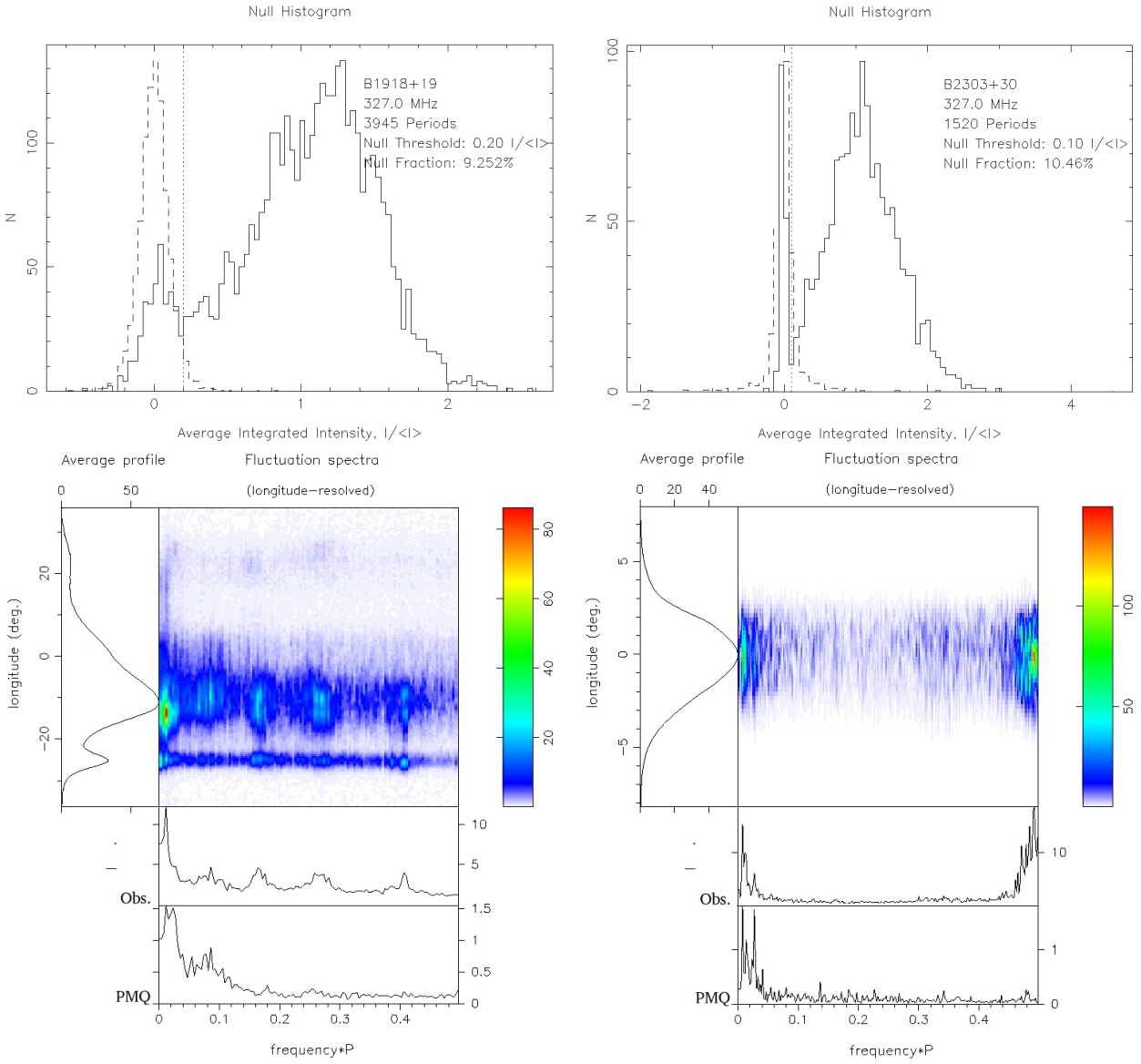

Figure 6. The top row shows typical pulse-energy histograms. The bottom rows show the average profile in the left panel, and in the right column: the LRF spectra in the top panel, the aggregate LRF spectra in the center, and the PMQ LRF aggregate spectra at the bottom. Pulsar B1918+19 on the left, B2303+30 on the right

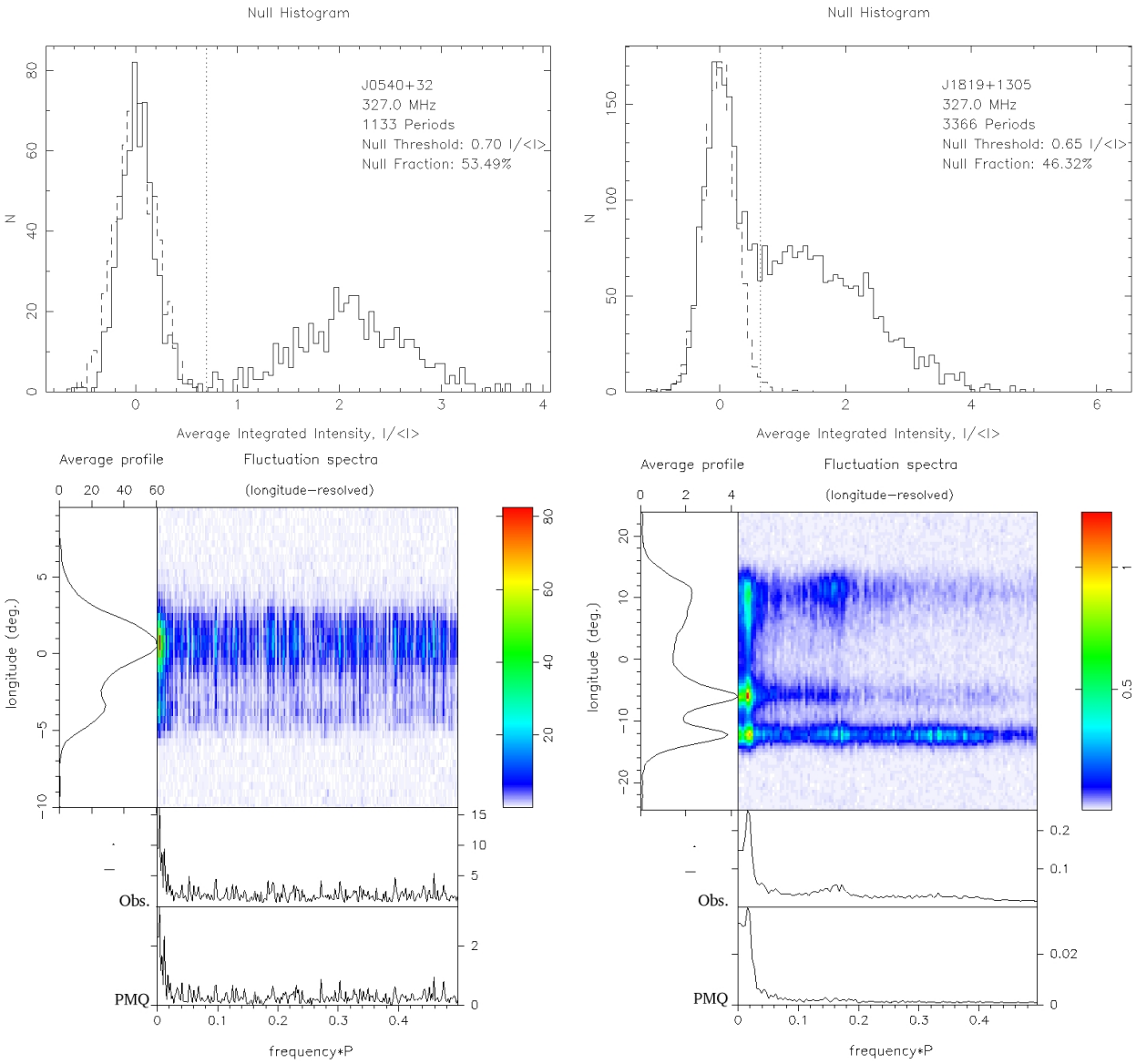

Figure 7. The top row shows typical pulse-energy histograms. The bottom rows show the average profile in the left panel, and in the right column: the LRF spectra in the top panel, the aggregate LRF spectra in the center, and the PMQ LRF aggregate spectra at the bottom. Pulsar J0540+32 on the left, J1819+1305 on the right

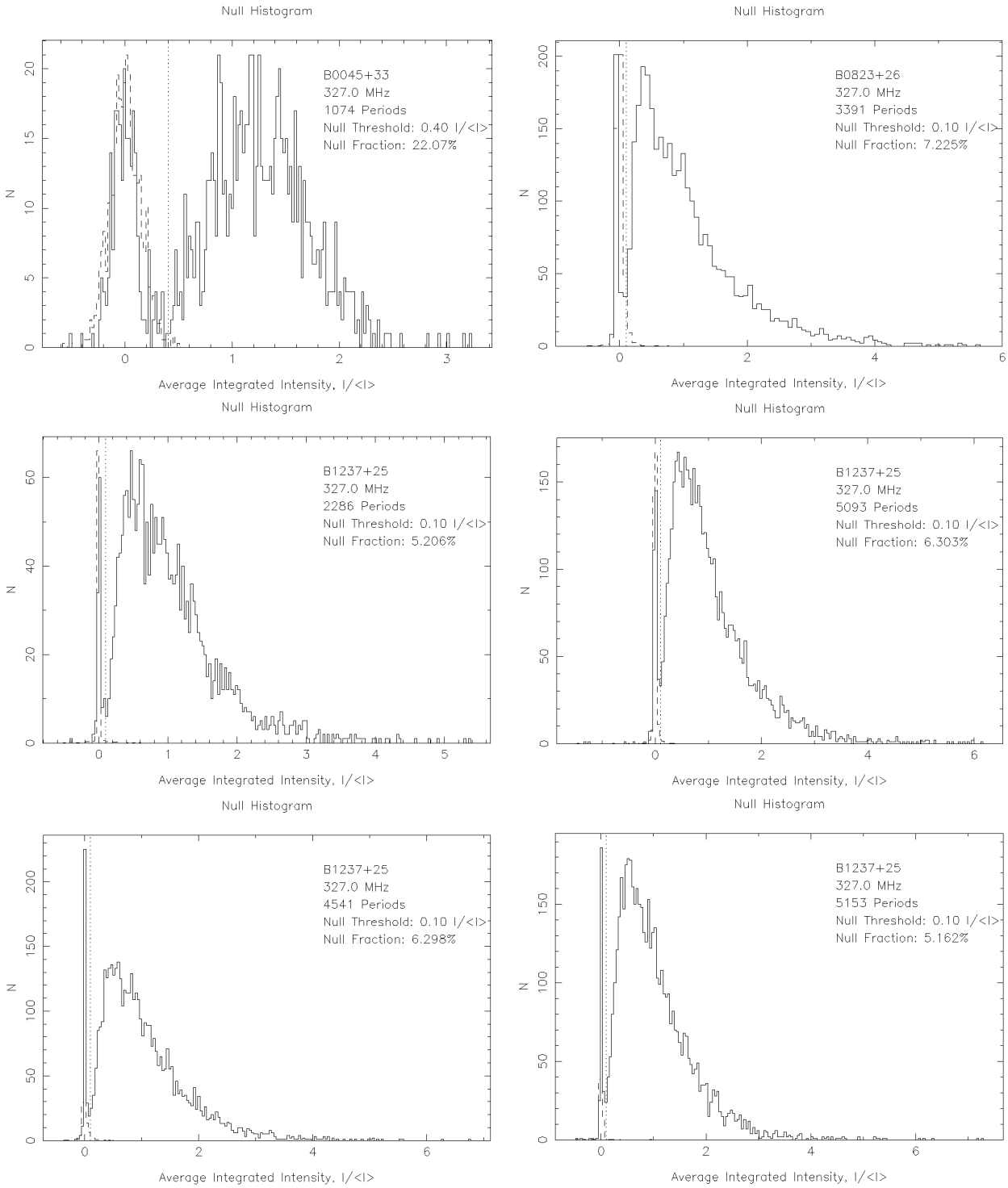

Figure 8. Typical pulse-energy histograms. Clockwise from the top left: B0045+33, B0823+26, B1237+25 dated 13 July 2003, B1237+25 dated 08 January 2005, B1237+25 dated 20 July 2003, B1237+25 dated 12 July 2003.

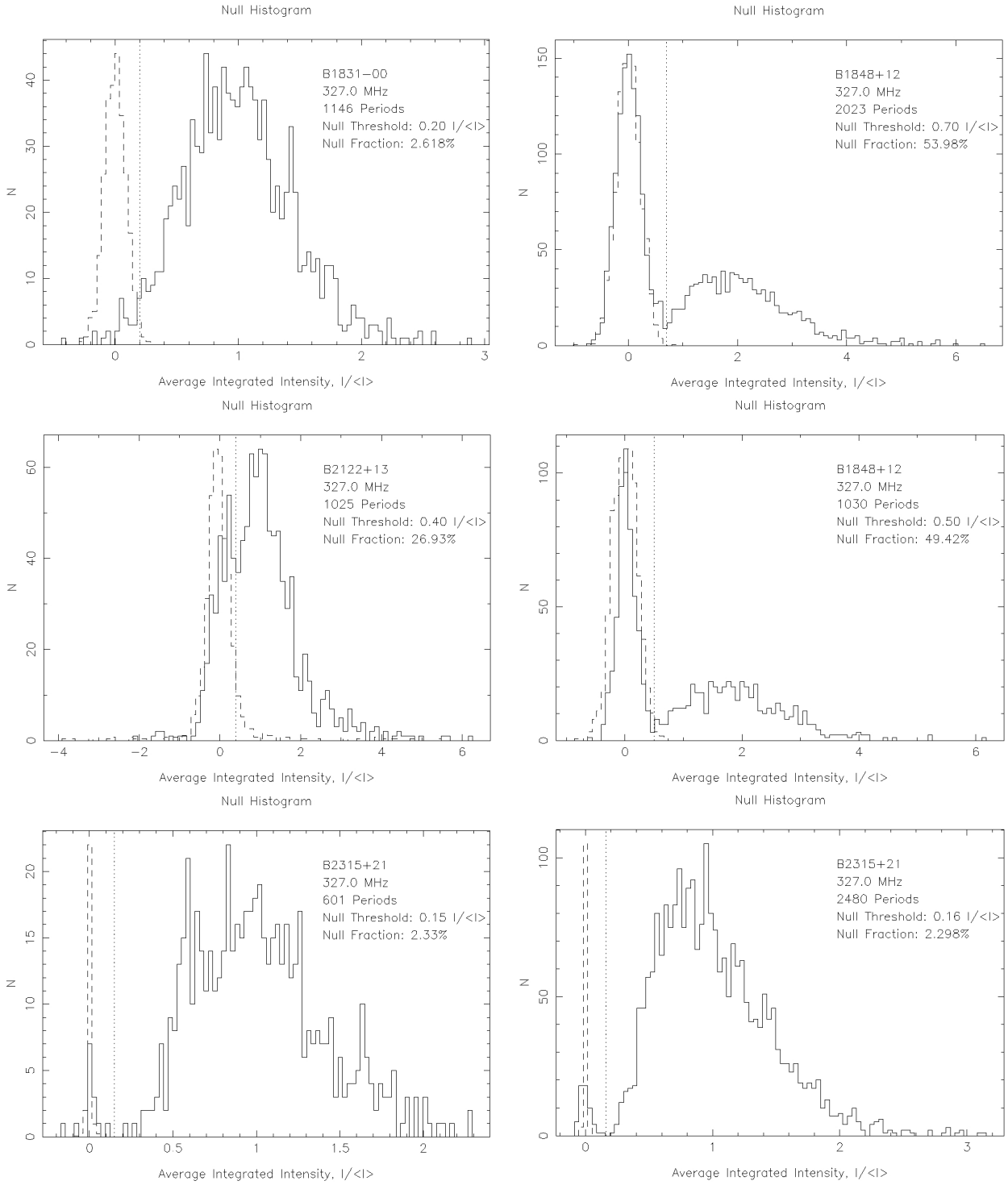

Figure 9. Typical pulse-energy histograms. Clockwise from the top left: B1831-00, B1848+12 dated 19 October 2003, B1848+12 dated 10 August 2006, B2315+21 dated 07 January 2005, B2315+21 dated 07 October 2003, B2122+13.